Theory of Series-Connected Distributed SIS Mixers with Ultra-Wide Instantaneous Bandwidth

C.-Y. Edward Tong, Raymond Blundell

***Abstract*— Series-connected distributed lumped element SIS mixers have emerged as a new generation of sensitive heterodyne submillimeter detectors which offer very wide instantaneous bandwidth. A formalism based on the transmission (ABCD) matrix is introduced to facilitate the simulation of this type of mixer with the Quantum Theory of Mixing. The simulations confirm that the IF bandwidth is very wide, up to at least 40 GHz. This agrees with our laboratory measurements in which good Y-factors are measured up to IF in excess of 20 GHz.**

***Index Terms*—Superconductor-insulator-superconductor mixers, distributed mixing, intermediate frequency bandwidth, submillimeter waves.**

I. Introduction

SERIES-CONNECTED SIS arrays offer many advantages over single SIS device or parallel connected SIS junctions. Such mixer arrays have higher input compression level and higher input impedance in addition to lower IF capacitance. However, at higher frequencies, the current flowing in the individual junctions of a series array may be of different phase. This presents a challenge to the design of an SIS mixer using series-connected array.

Recently, a compact mixer design based on a distributed 4-junction series array has successfully been implemented in the 400 GHz frequency range [1]. This mixer has demonstrated an exceptional wide Intermediate Frequency (IF) bandwidth of up to 20 GHz. In this paper, we describe how this novel mixer design can be modeled using the Quantum Theory of Mixing [2]. In particular, a formalism using an expanded transmission (ABCD) matrix is introduced so that the circuit response at each sideband can correctly be modeled, and the phase relation between the RF voltages and currents are preserved.

This mixer may also be simulated by the Supermix software [3, 4], which use a scattering matrix approach. The advantage of using the transmission matrix is that we can tie the circuit layout directly with the conversion matrix formalism in classical [5] and quantum mixer theory.

Manuscript received May 10, 2006.

C.-Y. E. Tong and R. Blundell are with the Harvard-Smithsonian Center for Astrophysics, 60 Garden St., Cambridge, MA 02138 USA. (e-mail: etong@cfa.harvard.edu, and rblundell@cfa.harvard.edu).

II. Mixer Layout

A photo of our novel mixer design is given in Fig. 1. Four SIS junctions are located on islands on the center conductor of coplanar waveguides. They are connected via short lengths of high impedance coplanar waveguides and low impedance microstrip sections. No impedance transformer is needed to feed the junction array. The distributed array is fairly well matched to a 35-ohm source impedance over a 20 – 25 % bandwidth. A nominal design calls for the use of 0.85 μm x 0.85 μm junctions having a critical current density of around 13 kA/cm^2.

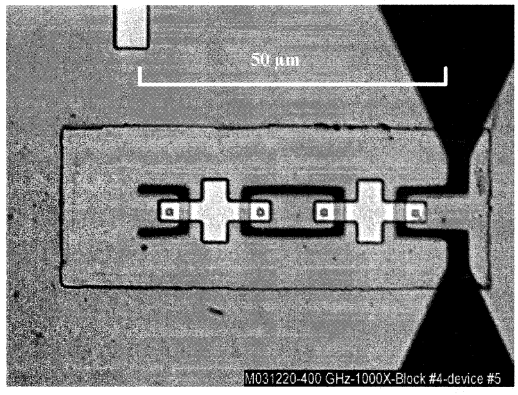

Fig. 1 Photograph of the series-connected distributed SIS mixer. The waveguide feed point is located on the right hand side of the photo. The 4 junctions are connected by sections of coplanar waveguide (CPW) and microstrip (the two white crosses).

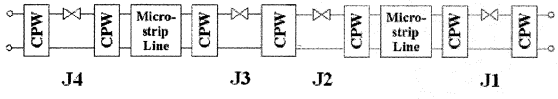

Fig. 2 Simplified schematic diagram of the SIS mixer circuit shown in Fig. 1. The junctions, J1, J2, J3 and J4 are in series positions along the artificial transmission line. The input to the circuit is to the right and the output after J4 is shorted.

A simplified schematic representation of the circuit is given in Fig. 2. It can be seen that the circuit can be broken into

cascaded blocks of circuit elements. The problem should be well described by the transmission (ABCD) matrix formalism in circuit theory.

III. Large Signal Analysis

Since the mixer under simulation works at around 400 GHz, the second harmonic frequency lies above the energy gap of Niobium. Furthermore, the individual series connected junctions are not tuned in parallel. Any harmonic current generated by the Local Oscillator (LO) drive is mostly shorted by the geometrical capacitance. This is particularly true since the $\omega_{LO}CR$ product of the junctions used is around 4. A three-frequency approximation is therefore sufficient to solve for the RF voltages impressed across the junctions by the LO.

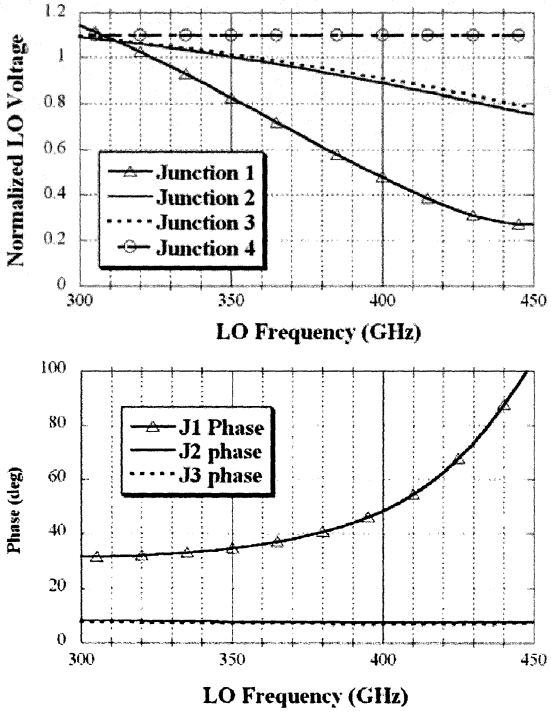

Fig. 3 Variation of the normalized LO voltage, α, as a function of the LO frequency for the 4 junctions in the array. The upper graph shows the amplitude of the voltages while the lower graph gives the phase relative to that of junction 4. In this calculation $\alpha_4 = 1.1$ is used as the starting solution.

Starting from an assumed RF voltage at the last junction in the array, we can derive the RF current flowing through the neighboring junction. In this calculation, we assume that the DC bias voltage across each junction equals 0.75 times the gap voltage. By inverting the non-linear current voltage relationship given by the Quantum Theory of Mixing, we can solve successively for the RF voltages across the other junctions in the array. The result of the large signal analysis is presented in Fig. 3. For this calculation, we have assumed that the normalized LO voltage across the last junction of the array, $\alpha_4 = eV_4 / h\nu_{LO}$, is equal to 1.1. We note that at the low end of the band, the amplitudes of voltages have similar values but at the high end, the first junction experience the least LO drive and the LO voltage is quite different in phase compared to other junctions.

IV. Expanded Transmission Matrix

Following standard mixer theory [2], we define the voltage and current vectors at any point in the mixer circuit as $\underline{v} = \begin{pmatrix} v_1 & v_0 & v_{-1} \end{pmatrix}^T$ and $\underline{i} = \begin{pmatrix} i_1 & i_0 & i_{-1} \end{pmatrix}^T$ respectively, where the subscripts 1, -1 and 0 denote the upper-side-band (USB), lower-side-band (LSB) and the IF respectively. In circuit theory, it is common to characterize a two-port network by a transmission (ABCD) matrix. We generalize it for use in our mixer simulation. The expanded transmission matrix of a mixer circuit element relates the input voltage and current vectors to the output voltage and current vectors of any two port network within the mixer circuit as:

$$\begin{pmatrix} \underline{V_{in}} \\ \underline{I_{in}} \end{pmatrix} = \begin{pmatrix} \mathbf{A} & \mathbf{B} \\ \mathbf{C} & \mathbf{D} \end{pmatrix} \cdot \begin{pmatrix} \underline{V_{out}} \\ \underline{I_{out}} \end{pmatrix} \qquad (1)$$

where **A**, **B**, **C** and **D** are 3 x 3 matrices. For a passive section of the mixer, the elements of the expanded transmission matrix are simply diagonal matrices, the entries of which are related to the individual elements of the single-frequency transmission matrices $\mathbf{T}_i$ for i = 1, 0 and -1. Thus, in equation (1), for $X = A, B, C$ or D:

$$\mathbf{X} = \begin{pmatrix} X_1 & 0 & 0 \\ 0 & X_0 & 0 \\ 0 & 0 & X_{-1}^* \end{pmatrix} \qquad (2)$$

and

$$\mathbf{T}_i = \begin{pmatrix} A_i & B_i \\ C_i & D_i \end{pmatrix} \qquad (3)$$

It should be noted that all LSB entries are the conjugate of the single frequency transmission matrix representation, consistent with classical mixer theory.

Equation (1) embeds the circuit description for all the sidebands involved in the mixer simulation. In the case of the series-connected mixer element, the expanded transmission matrix that describes it would be

$$\begin{pmatrix} \underline{V_{in}} \\ \underline{I_{in}} \end{pmatrix} = \begin{pmatrix} \mathbf{I} & \left(\mathbf{Y}_c(\alpha) + \mathbf{Y}_j \right)^{-1} \\ \mathbf{0} & \mathbf{I} \end{pmatrix} \cdot \begin{pmatrix} \underline{V_{out}} \\ \underline{I_{out}} \end{pmatrix} \qquad (4)$$

where **I** is the identity matrix, **0** is the null matrix and $\mathbf{Y}_j$ is the diagonal matrix that gives the susceptance due to the junction's geometrical capacitance at the three sideband frequencies. $\mathbf{Y}_c(\alpha)$ is the conversion admittance matrix given by the Quantum Theory of Mixing for each individual junction as a function of the normalized LO voltage, α, derived in the large signal analysis. Since the LO voltages

across the different junctions have different phases, the entries of the conversion matrix have to be multiplied by phase factors given in [5]. We have also used the low-IF assumption in formulating the conversion matrices, without considering the quantization effects at high IF. This approximation is valid for IF less than $F_{LO}/10$ [7]. Consequently, we limit the maximum IF to be 40 GHz in our simulation.

The expanded transmission matrix formalism creates a framework in which we can integrate passive transmission line elements with mixing elements. This is a very powerful tool for the simulation of the series-connected distributed mixer. The formalism can easily be generalized to simulate 5-port mixers in which harmonic effects are important. In that case, the entries to the expanded transmission matrix would be 5 x 5 matrices.

Once the RF voltages across individual junctions are solved in the large-signal analysis, we can formulate the expanded transmission matrix of the entire mixer circuit by matrix multiplication. The final step is to apply the boundary condition, which is $\underline{V_{out}} = 0$ for our mixer layout because one side of the last junction is shorted to ground. Referring to equation (1), we can see that the final conversion admittance matrix of the mixer array is:

$$\mathbf{Y}_{\text{final}} = \mathbf{D}_{\text{final}} \cdot \mathbf{B}_{\text{final}}^{-1} \qquad (5)$$

By adding the appropriate embedding admittances to $\mathbf{Y}_{\text{final}}$, the conversion loss of the mixer and the port impedances can be solved.

V. Noise Analysis

The shot noise generated at each junction is transformed by the entire mixer circuit before making its way to the mixer ports. Assuming that the noise generated at each device is not correlated with that generated at other devices, we can use the theorem of superposition to sum the noise power delivered to the IF port from the individual junctions, activating one junction at a time.

Referring to Fig. 4, we assume that a noise current source, $\underline{\langle In_j \rangle}$, is put across the junction j (j = 1, 2, 3 or 4). Note that the noise current is also expressed in a vector form because it has components at all three sidebands of interest. In order to solve for the noise power delivered to the embedding impedance due to $\underline{\langle In_j \rangle}$, we have to first calculate the expanded transmission matrix of the network lying between the source impedance and the device (marked "Front section" in the figure) and that of the network lying beyond the junction (marked "Back section"). Once the expanded transmission matrices for the front and back sections are established, we can solve for the noise impedance matrix that relates the noise voltage induced across the embedding impedance, $\underline{\langle Vne_j \rangle}$ to $\underline{\langle In_j \rangle}$:

$$\underline{\langle Vne_j \rangle} = \mathbf{Zn}_j \cdot \underline{\langle In_j \rangle} \qquad (6)$$

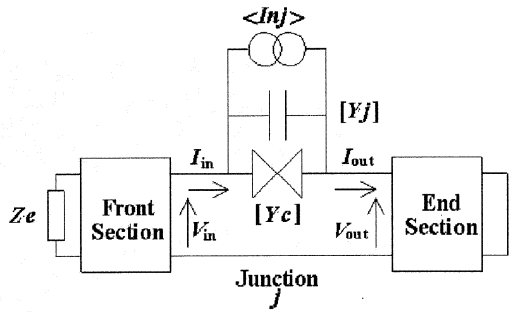

Fig. 4 A schematic representation of the mixer circuitry seen by the shot noise source associated with Junction j (j = 1, 2, 3 or 4). The SIS element is modeled by a capacitance matrix $[Yj]$ in parallel to its conversion matrix $[Yc]$.

The total mean-squared noise voltage delivered to the IF terminal is the sum of the contributions from all four junctions. The algebraic expression is:

$$\underline{\langle V_N^2 \rangle} = \sum_{j=1}^{4} \sum_{k=-1}^{1} \sum_{k'=1}^{1} \left(\mathbf{Zn}_j\right)_{0,k} \left(\mathbf{Zn}_j\right)_{0,k'}^{*} \left(\mathbf{H}_j\right)_{k,k'} \qquad (7)$$

In the above equation $\mathbf{H}_j$ is the current correlation matrix given by the Quantum Theory of Mixing. Knowing the single-side-band conversion gain of the mixer, L_{SSB}, one can establish the single-side-band noise temperature of the mixer due to shot noise effects:

$$k_B T_{SSB} = L_{SSB} \,\mathrm{Re}(Y_e(\omega_0)) \langle V_N^2 \rangle \qquad (8)$$

Where k_B is the Boltzmann constant and $Y_e(\omega_0)$ is the embedding admittance at the IF. For double-side-band noise temperature, the average value of the sum of the conversion losses in both side-bands is used.

VI. Simulation Results

We first performed a simulation of the mixer performance at a fixed IF of 5 GHz. It is found that the conversion loss of the mixer is relatively insensitive to LO drive when the normalized LO voltage across junction 4 reaches a value of 1.1. Referring to Fig. 5, the conversion losses of the mixer for both sidebands are quite flat from 320 to 420 GHz. This represents a bandwidth of about 25%, comparable to transformer-matched SIS mixer.

Then, we fix the LO frequency to the middle of the band, at 370 GHz. But we vary the IF from 2 GHz to 40 GHz. The results are plotted in Fig. 6. The calculated conversion loss of the mixer only drops by about 1 dB over this IF range. Clearly, the simulation demonstrates that our series-connected distributed mixer design offers an ultra-wide IF bandwidth.

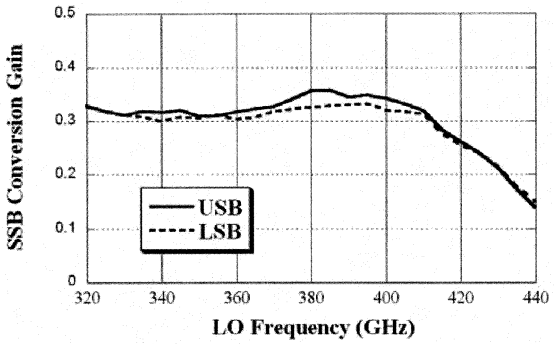

Fig. 5 Single-side-band Conversion Gain of the SIS mixer as a function of LO frequency. The IF is at 5 GHz. We also assume that $\alpha_4 = 1.1$ and the bias voltage to be 0.75 Vgap.

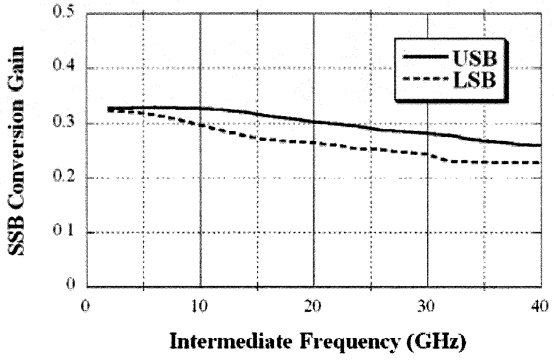

Fig 6 Single-side-band conversion gain of the receiver as a function of the IF for an LO frequency of 370 GHz.

The double-side-band mixer noise temperature is also simulated. The result is plotted in Fig. 7. We can see that for a mixer with a low leakage current, the mixer noise temperature stays below the quantum limit ($h\nu/k \sim 18$ K at 370 GHz). The results of simulation agree with noise temperature measured in the lab. Preliminary measurements at an LO of 355 GHz have yielded double-side-band receiver noise temperatures below 80 K for IF between 15 and 20 GHz. We are currently working on the improvement of the IF circuitry to increase the bandwidth of measurement.

VII. Conclusion

A three-frequency expanded transmission matrix has been introduced to facilitate the modeling of the series-connected SIS junction array. This formalism offers a unified description of the frequency mixing action of the SIS and the passive transmission networks linking these series-connected devices, at all the three frequencies under consideration (signal, image and IF). Our simulation confirms that the series-connected distributed SIS mixer possesses a flat RF response over a 25% bandwidth, and at the same time offering an exceptionally wide instantaneous bandwidth of up to 40 GHz. The intrinsic noise temperature of this class of mixer lies also below the quantum limit.

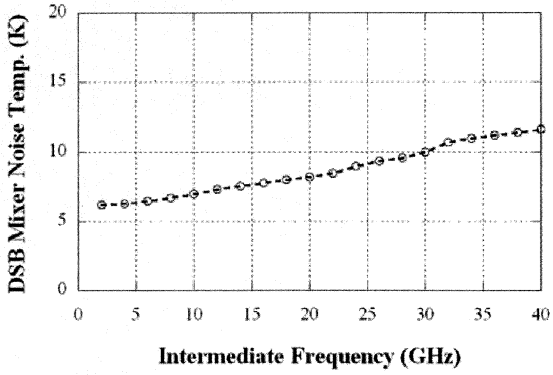

Fig. 7 Double-side-band mixer noise temperature of the SIS mixer as a function of IF for an LO frequency of 370 GHz.

References

[1] C.E. Tong, R. Blundell, K.G. Megerian, J.A. Stern, S.-K. Pan, and M. Popieszalski, "A distributed lumped-element SIS mixer with very wide instantaneous bandwidth," *IEEE Trans. Appl. Supercond.*, vol. 15(2), pp. 490-494, June 2005.

[2] J.R. Tucker, and M.J. Feldman, "Quantum detection at millimeter wavelengths," *Rev. Modern Phys.*, vol. 57, pp. 1055-1113, Oct. 1995.

[3] J. Ward, F. Rice, G. Chattopadhyay, and J. Zmuidzinas, "SuperMix: A flexible software library for high-frequency circuit simulation, including SIS mixers and superconducting elements," in *Proc. 10th Int. Symp. Space THz Tech.*, Charlottesville, VA, *Ed.* T. Crowe, pp. 268-280, March 1999.

[4] F. Rice, J. Ward, *private communications,* 2006

[5] C.-Y. E. Tong, R. Blundell, B. Bumble, J.A. Stern, and H.G. LeDuc, "Distributed mixing in a non-linear transmission line at sub-millimeter wavelengths," *IEEE Trans. Appl. Supercond,* vol. 7, pp. 3597-3600, Jun 1997.

[6] S.-K. Pan, and A.R. Kerr, "SIS mixer analysis with non-zero intermediate frequencies," in *Proc. 7th Int. Symp. Space THz Tech.*, Charlottesville, VA, *Ed.* T. Crowe, pp. 195-206, March 1996.

[7] C.E. Tong, L. Chen, and R. Blundell, "Theory of distributed mixing and amplification in a superconducting quasi-particle nonlinear transmission line," *IEEE Trans. Microwave Theory & Tech.*, vol. 45, pp. 1086-1092, Jul. 1997.